

Received: 2016.03.22  
Accepted: 2016.06.13  
Published: 2016.10.18

# Synthesis and Biological Evaluation of a New Nitroimidazole-<sup>99m</sup>Tc-Complex for Imaging of Hypoxia in Mice Model

Authors' Contribution:  
Study Design A  
Data Collection B  
Statistical Analysis C  
Data Interpretation D  
Manuscript Preparation E  
Literature Search F  
Funds Collection G

CD 1 **Qing Zhang**  
D 1 **Qing Zhang**  
BC 1 **Yanxing Guan**  
F 1 **Shaozheng Liu**  
D 1 **Qingjie Chen**  
AG 2 **Xiangmin Li**

1 Department of Nuclear Medicine, The First Affiliated Hospital of Nanchang University, Nanchang, Jiangxi, P.R. China  
2 Jiangxi-OAI Joint Research Institute, Nanchang University, Nanchang, Jiangxi, P.R. China

**Corresponding Author:** Xiangmin Li, e-mail: xiangminll@126.com  
**Source of support:** Departmental sources

**Background:** This study was specifically designed to develop a new <sup>99m</sup>Tc compound with 3-amino-4-[2-(2-methyl-5-nitro-1H-imidazol)-ethylamino]-4-oxo-butylate (5-ntm-asp) and to verify whether this compound is feasible to be a radiopharmaceutical for hypoxic tumors.





**Material/Methods:** Metronidazole derivative 5-ntm-asp was synthesized and then radio-labeled by Na [<sup>99m</sup>TcO<sub>4</sub>], forming <sup>99m</sup>Tc-5-ntm-asp. Another two complexes of <sup>99m</sup>Tc-2- and <sup>99m</sup>Tc-5-nitroimidazole-iminodiacetic acid (<sup>99m</sup>Tc-2-ntm-IDA and <sup>99m</sup>Tc-5-ntm-IDA) were also synthesized based on previous studies. Physicochemical properties (stability, lipophilicity, protein binding) of the compounds were compared, and we also assessed the accumulation status of the compounds within A549 cells under both hypoxic and aerobic conditions. Distribution of the complex was also studied *in vivo* using BALB/c nude mice that were injected with A549 cells.

**Results:** Compared with <sup>99m</sup>Tc-2-ntm-IDA and <sup>99m</sup>Tc-5-ntm-IDA, <sup>99m</sup>Tc-5-ntm-asp was more stable in both phosphate-buffered saline (PBS) buffer and human plasma (*P*<0.05). Besides that, <sup>99m</sup>Tc-5-ntm-asp offered lower lipophilicity and protein-binding rate than the two complexes (*P*<0.05). During assessment of hypoxic uptake status and high hypoxic/aerobic ratio in mice injected with A549 cells, <sup>99m</sup>Tc-5-ntm-asp exhibited a more favorable profile than <sup>99m</sup>Tc-2-ntm-IDA and <sup>99m</sup>Tc-5-ntm-IDA, including uptake ratio of tumor/blood and uptake ratio of tumor/muscle.

**Conclusions:** With overall consideration of physicochemical properties and biological uptake behavior, it is feasible to use <sup>99m</sup>Tc-5-ntm-asp as an imaging agent for tumor hypoxia.

**MeSH Keywords:** Cell Hypoxia • Metronidazole • Potassium Magnesium Aspartate • Technetium

**Full-text PDF:** <http://www.medscimonit.com/abstract/index/idArt/898659>

 3911  4  9  29



## Background

Hypoxia is defined as a status in which cells have deficient oxygen supply, and it may affect living functions of cells. Several risk factors for hypoxia have been identified, including cancer, diabetes, infection/wound healing, and cardiovascular/cerebrovascular diseases [1]. Early detection of tumor hypoxia is extremely important since it has significant influence on those patients who may benefit from hypoxia-directed therapy [1]. Apart from that, tumor hypoxia may cause resistance to both radiotherapy and chemotherapy, and it is associated with poor prognosis [2]. As a result, identification and quantification of tumor hypoxia may assist in predicting both clinical and diagnostic outcomes [3]. Hypoxia markers have been extensively investigated over the past decade, and several potential radiopharmaceuticals along with some bio-reductive compounds have been proved to be valuable markers for tumor hypoxia as they may selectively diminish hypoxic tissues in order to activate intermediates that bind with intracellular molecules [4]. Therefore, the main objective for detecting tumor hypoxia is to find appropriate molecules that are able to target hypoxic tissues.

Nitroimidazoles are classified as antibiotic drugs that are categorized based on the location of the nitro functional group on the imidazole ring and xanthine oxidase. Furthermore, nitroimidazoles are widely explored and accepted for targeting hypoxic tissues [5]. Xanthine oxidases play a catalytic role in the reaction and may further reduce cellular components under hypoxic conditions, while the supply of oxygen is able to obtain electrons derived from the nitro radical anion under normal conditions. Therefore, we suspected that derivatives of radiolabeled nitroimidazoles are likely to serve as hypoxia markers [4].

Nitroimidazoles as molecules for targeting hypoxic tissues have been investigated in many studies, and differently substituted nitroimidazoles, i.e., 2-, 4- and 5-nitroimidazole, have variations in their physicochemical properties. For instance, Chu et al. reported that <sup>99m</sup>Tc-BATO complex containing 4-nitroimidazole can selectively retain hypoxic tissues [3]. Furthermore, Evans et al. conducted a study on the development of <sup>18</sup>F-labeled 2-nitroimidazole as a non-invasive imaging modality for hypoxia, and they concluded that this compound was a desirable radiotracer for non-invasive imaging of tumor hypoxia [6]. Nevertheless, these hypoxia markers contained several limitations such as selectivity deficiency and excessive background signal of blood [5]. As a result of this, alternative compounds that are able to identify tumor hypoxia and overcome these limitations may provide additional assistance [7]. The 5-nitroimidazole metronidazole with high affinity for hypoxic tumors *in vitro* and *in vivo* is one of the potential hypoxia makers, and it is considered to be the original material for preparing <sup>99m</sup>Tc radiopharmaceuticals [8].

Technetium is a kind of transition metal, which is a major challenge for devising radiopharmaceuticals that contain desirable properties *in vivo* [9]. Moreover, it has been acknowledged that <sup>99m</sup>Tc has a critical role in nuclear medicines that are used for disease diagnosis, and it is valued in several chemical diagnostic scans that are conducted in hospitals [9]. On top of that, <sup>99m</sup>Tc has been verified as an alternative for nuclear imaging due to its low production cost compared with other elements such as <sup>18</sup>F and <sup>123</sup>I [5]. Previous studies have concluded that combining bio-reductive pharmacophore with <sup>99m</sup>Tc is able to form highly stable complexes *in vivo* and *in vitro* [10]. Additionally, <sup>99m</sup>Tc contains a newly available chelating moiety for creating <sup>99m</sup>Tc radiopharmaceuticals that can be used to design hypoxic tissue markers [11].

In this study, we synthesized <sup>99m</sup>Tc-5-ntm-asp and monitored radiopharmaceuticals using high-pressure liquid chromatography (HPLC) and mass spectrometry (MS) analysis. We also analyzed and compared several main biological and physicochemical properties of <sup>99m</sup>Tc-5-ntm-asp, <sup>99m</sup>Tc-2-ntm-IDA, and <sup>99m</sup>Tc-5-ntm-IDA *in vitro* and *in vivo*. Comparison of these properties, as reflected by the compounds, enabled us to evaluate the feasibility of <sup>99m</sup>Tc-5-ntm-asp as a promising hypoxia-targeting radiopharmaceutical in clinical practice [8].

## Material and Methods

### General

Metronidazole, phthalic diamide, triphenylphosphine, diisopropyl azodiformate (DIPA), Boc-L-aspartic acid 1-benzyl ester (Boc-Asp-OBzl), diethyl chlorophosphate (DECP), and trifluoromethanesulfonic acid (TfOH) were purchased from Sigma Aldrich, USA. Diethylene oxide, ether, hydrobromic acid, triethylamine, dichloromethane, magnesium sulfate, trifluoroacetic acid (TFA), and baking soda were purchased from Fluka, Germany. Na[<sup>99m</sup>TcO<sub>4</sub>] was obtained from a generator purchased from China Isotope and Radiation Corporation laboratory (Beijing). All other basal reagents were purchased from VWR International, USA. Pre-coated plates of silica gel 60 F254 (Merck, India) were obtained for the purpose of thin layer chromatography (TLC). HPLC analyses were carried out under the JASCO PU 2080 Plus dual pump HPLC system (Waters, USA). C18 reversed phase HiQ Sil column (4×250 mm) was used for separating various components in the process of radioactive preparation. Mass spectra were performed with an API 300 LC/MS Trap mass spectrometer (ABI, USA). Radioactivity was assessed using a scintillation counter for gamma (1470-002, PerkinElmer, USA).

Human lung cancer cell line A549 was purchased from the Institute of American Type Culture Collection (ATCC, USA).

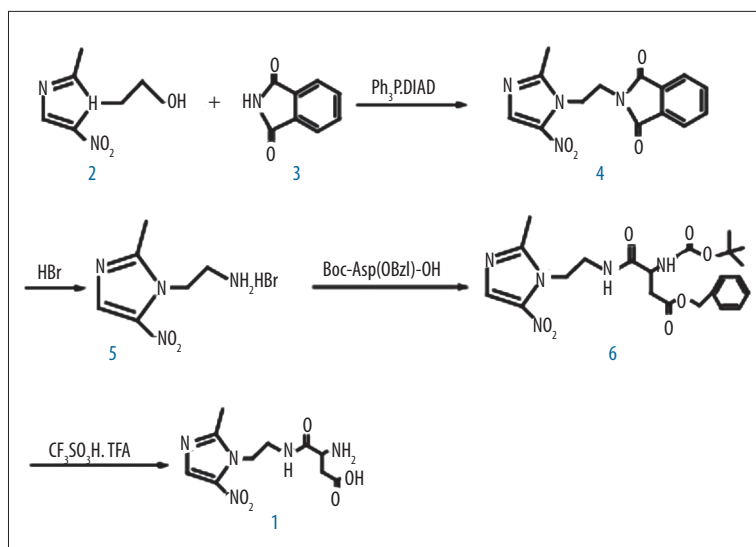


**Figure 1.** Synthesis of 5-nitroimidazole-asparagine (compound 1).

Cells were cultured at 37°C in Dulbecco's Modified Eagle Medium (Gibco, Carlsbad, California) with 10% fetal bovine serum (Gibco, Carlsbad, California) in an incubator that contained 5% CO<sub>2</sub>. Male BALB/c nude mice (Laboratory Animal Center of Southern Medical University) with an average age of 4 weeks and weight of 16–18 g were obtained in order to build tumor growth models. All mouse experiments complied with the Guidance for Care and Usage of Laboratory Animals and were adopted by the National Cancer Institute Animal Care and Use Committee.

## Synthesis of compounds

### Synthesis of 2- and 5-nitroimidazole-iminodiacetic acid (IDA)

Synthesis and characterization of 2- and 5-nitroimidazole-IDA were conducted based on earlier reports [1], and the structures are shown in Supplementary Figure 1.

### Synthesis of 3-amino-4-[2-(2-methyl-5-nitro-1H-imidazol-1-yl)ethylamino]-4-oxo-butanoic acid (5-nitroimidazole-asparagine, 1)

As suggested by Figure 1, synthesis of 5-nitro-asp was implemented using a four-step reaction.

### Synthesis of N-[2-(2-methyl-5-nitro-1H-imidazol-1-yl)ethyl]-phthalimide (4)

Metronidazole (**2**, 4.0 g), phthalic diimide (**3**, 5.15 g), and triphenylphosphine (9.18 g) were dissolved in dry diethylene oxide (200 mL). After these compounds were cooled to 0°C, a solution of DIAD (15.2 g) dissolved in diethylene oxide (20 mL) was slowly added to the former mixture with whisking. Then incubation was carried out at room temperature for 4 hours. After that, this solution was removed using a rotary evaporator,

and white solid (compound **4**, 5.5 g) was separated out and washed with isopropanol (100 mL).

### Synthesis of 2-(2-methyl-5-nitro-1H-imidazol-1-yl)-hydrogen bromide (5)

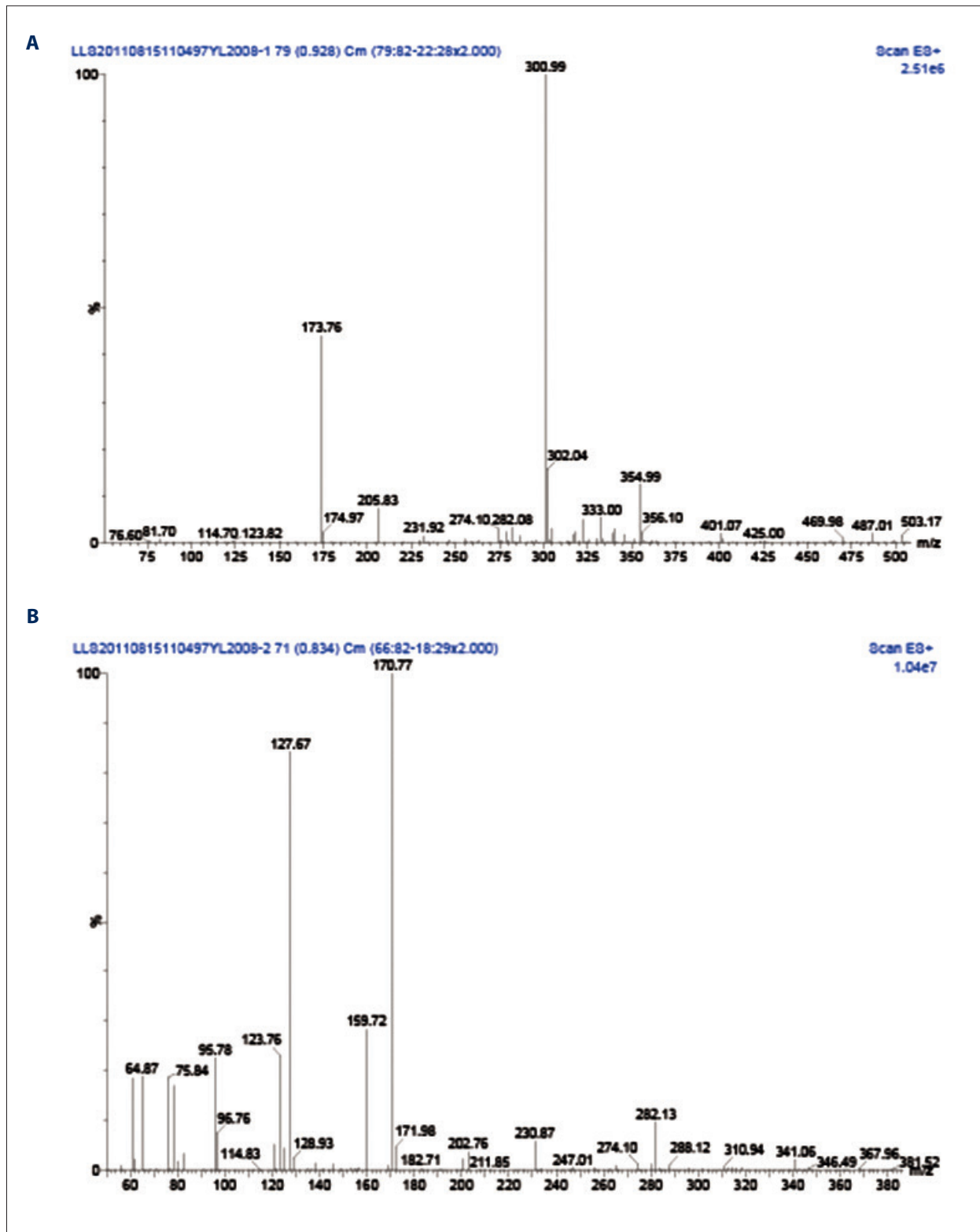
Compound **4** (3.0 g) was dissolved in 30% hydrobromic acid (110 mL), and this mixture was heated to reflux for 16 hours and then concentrated with reduced pressure. Once the mixture was washed twice with dry ethyl alcohol (50 mL) followed by a final wash with dry diethyl, yellow solid (compound **5**, 2.6 g) was separated out and washed with ethanol (100 mL).

### L3 Synthesis of 3-(butyl-oxygen-carbonyl-amino)-4-[2-(2-methyl-5-nitro-1H-imidazol-1-yl)ethylamino]-4-oxo-benzyl butyrate (6)

Boc-Asp-OBzl (0.33 g), compound **5** (0.25 g), and triethylamine (0.3 mL) were dissolved in dry dichloromethane (5 mL), and this mixture was cooled to 0°C. DECP (0.33 mL) was added to the solution and mixed for 1 hour. This solution was mixed for another 3 hours once room temperature was reached, and then it was washed with water. The organic layer was separated out and washed with dry magnesium sulfate. Finally, compound **6** (0.1 g) was purified using the method of column chromatography.

### Synthesis of 3-amino-4-[2-(2-methyl-5-nitro-1H-imidazol-1-yl)ethylamino]-4-oxo-butanoic acid (5-nitroimidazole-asparagine, 1)

Compound **6** (0.5 g) was dissolved in TFA (4 mL) and mixed under an ice-salt bath. Then TfOH (4 mL) was slowly added to the solution over 20 minutes, and incubation was performed under the ice-salt bath for 4-5 hours. After that, dry diethyl (10 mL) was slowly added to the mixture under the ice-salt bath for another 10 minutes. Supernatant was separated and



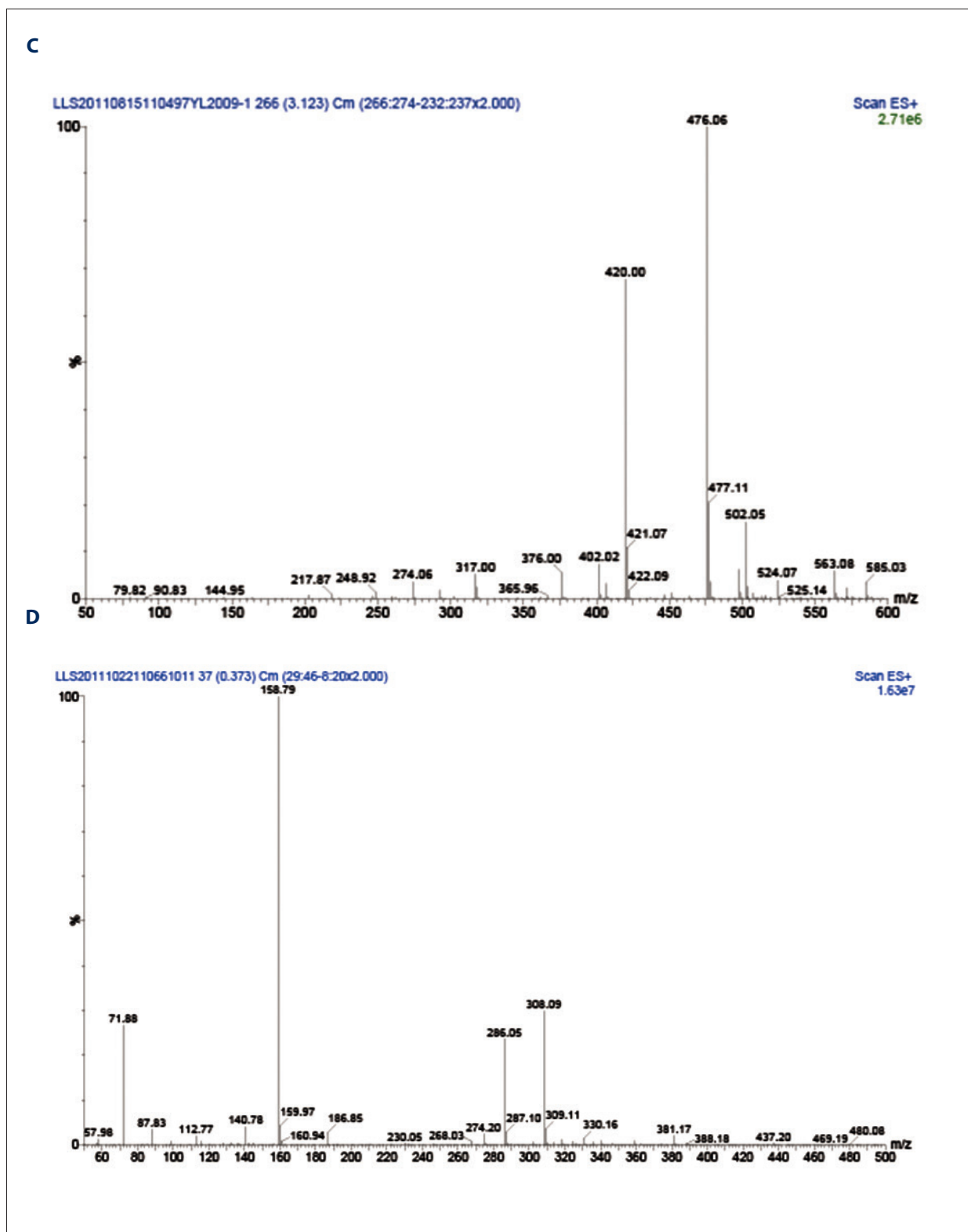
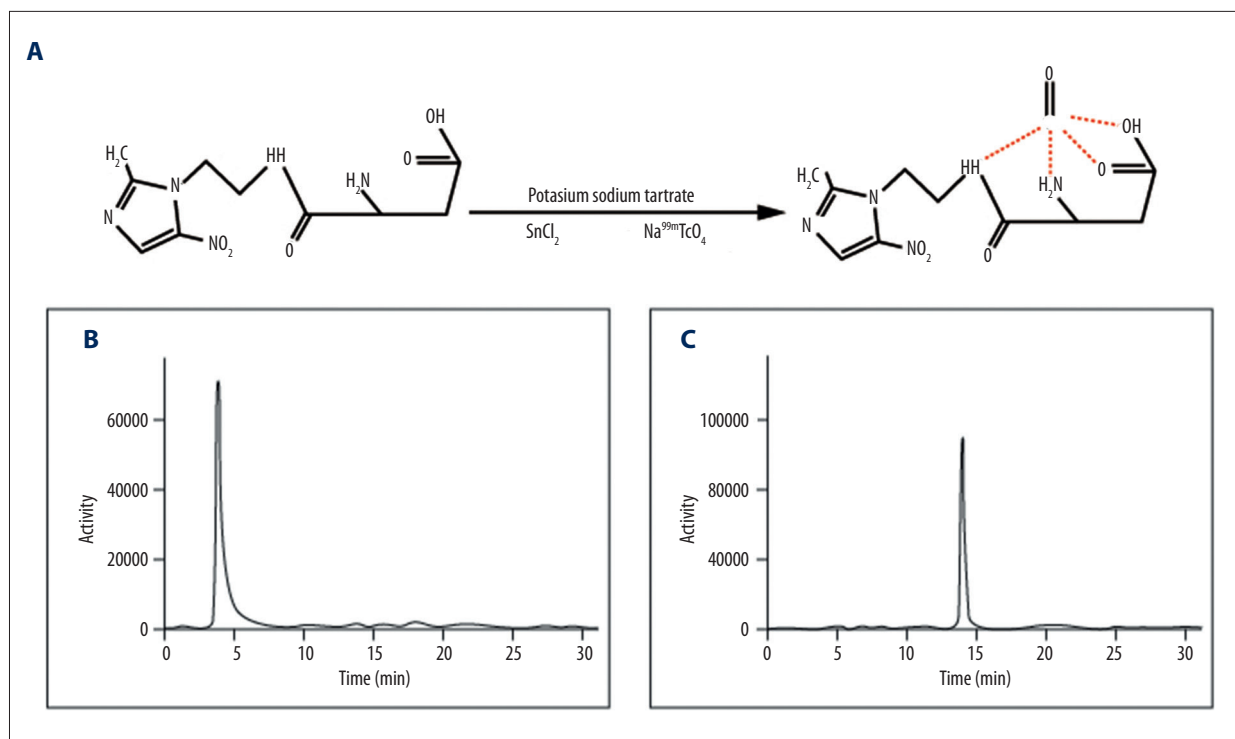


Figure 2. Mass spectrometry analyses of compound 4 (A), compound 5 (B), compound 6 (C), and compound 1 (D).



**Figure 3.** Radiolabeling route (A) and typical HPLC chromatograms for Na[<sup>99m</sup>TcO<sub>4</sub>] (B) and <sup>99m</sup>Tc-5-nitroimidazole-asparagine (C).

washed 5-7 times with dry diethyl, and removed using a rotary evaporator. Finally, the solid was dissolved in purified water (1 mL) and its pH value was adjusted within the range of 7–8 using baking soda. Compound **1** (0.2 g) was purified using the approach of column chromatography (Sephadex G-10)

#### MS analysis

Once purification of the synthesized 5-ntm-asp was completed, intermediate and final compounds were characterized by MS. As shown in Figure 2, MS analyzed the presence of *m/z* fragments that were associated with an expected molecular ion ([*M*+*H*<sup>+</sup>] ion peaked at *m/z* 300.99 for compound **4**, 170.77 for compound **5**, 476 for compound **6**, and 286 for compound **1**).

#### Radiolabeling

##### <sup>99m</sup>Tc complex preparation

The radiolabel of ntm-IDA was achieved based on earlier reports [1], and synthesis of <sup>99m</sup>Tc-ntm-asp complex is shown in Figure 3A.

The solution of compound **1** (0.2 mL, 1 g/L) was mixed with potassium sodium tartrate solution (0.025 mL, 1g/L). The pH value of the mixture was adjusted to 7.0-7.4 using phosphate buffer (0.1 mol/L, pH 7.4). Then fresh SnCl<sub>2</sub> (0.01 mL, 1g/L) dissolved in HCl (0.01 mol/L) and fresh Na[<sup>99m</sup>TcO<sub>4</sub>] solution (0.1

mL, 37 MBq) were added into the mixture. Mixing was performed at 75°C for 15 min.

#### HPLC analysis

Finally, purities of the radiochemical precursor Na[<sup>99m</sup>TcO<sub>4</sub>] and <sup>99m</sup>Tc-ntm-asp complex were evaluated using the method of HPLC. The retention times of these two compounds were 4.0 min and 14.0 min, respectively (Figure 3B, 3C).

#### Physicochemical characteristics of complexes

##### Stability in vitro

The three studied <sup>99m</sup>Tc-complexes (100 μL, 7.4 MBq) were incubated in phosphate-buffered saline (PBS) at room temperature for up to 4 hours. Then, the radiochemical purities were calculated using the HPLC approach under general experimental conditions.

##### Serum stability in vitro

The three studied <sup>99m</sup>Tc-complex (100 μL, 7.4 MBq) was added to 900 μL of human serum and then incubated for up to 4 hours at 37°C. After incubation was carried out for 1, 2, and 3 hours, samples (200 μL) were extracted from the original complexes and analyzed using the HPLC approach once the proteins were precipitated using ethanol (200 μL).

### Partition coefficient (lipophilicity)

Firstly, <sup>99m</sup>Tc-complex (100 µL), water (900 µL), and n-octanol (1000 µL) were mixed together using a vortex mixer. Secondly, this mixture was added to MicroSpin G-50 columns and then centrifuged at 3500 g for 3 min. After 800 µL of octanol was withdrawn and 800 µL of water was added, the mixture was blended and centrifuged again. Finally, radioactivity results were calculated in a NaI (Tl) counter and expressed as  $\text{Log } (P_{o/w}) = \text{Log} [( \text{counts in octanol} ) / ( \text{counts in water} )]$ .

### Protein binding

The three studied <sup>99m</sup>Tc-complexes (100 µL, 7.4 MBq) were added to 900 µL of human plasma, and then the mixture was incubated at 37°C for up to 2 hours. Samples (50 µL) were extracted from the original mixture once incubation had been carried out for 2 hours. After that, the extracted samples were added into G-50 columns and centrifuged at 2000 g for 3 min. Finally, elute was collected, and radioactivity was calculated in a NaI (Tl) counter. Protein-binding results were expressed as a percentage of elute activity over column activity.

### Biological evaluation

#### Cell uptake studies in vitro

A549 cells were grown in fresh medium until the desired cell density (10<sup>6</sup>/mL) was achieved. Once cells were equilibrated in glass vials at 37°C under two separate gas conditions – hypoxia exposure (95% N<sub>2</sub> +5% CO<sub>2</sub>) and aerobic exposure (95% air +5% CO<sub>2</sub>) – they were added with three types of <sup>99m</sup>Tc-complexes (200 µL, 14.8 MBq) whose final radioactivity was 0.25 MBq/mL. Samples of 0.2 mL were separated from the original complex and placed in another tube in which the same gas condition was applied to cells. This procedure was replicated at various time points (5 min, 0.5 h, 1 h, 2 h, 4 h). Then cells were separated from samples using 1500 r/min centrifugation for another 5 minutes. The radioactivity of supernatant (180 µL) was counted as Cs, whereas the radioactivity of the remaining samples (20 µL) was counted as Cr. Results of radioactivity uptake in cells were calculated as:  $(\text{Cr}-\text{Cs}/9) / (\text{Cr}+\text{Cs})$ .

#### Cell uptake in vivo

A549 cells were subcutaneously injected into the neck of mice (1×10<sup>6</sup> cells for each mouse). Once tumor nodules (0.5–1.5 cm, 75–1200 mg) were successfully developed in the mice, three groups of mice were separately injected with the three studied <sup>99m</sup>Tc-complexes (100 µL, 7.4 MBq). Cervical dislocation treatment was carried out for each mouse, and tissues along with organ samples were collected from mice at various time points (30 min, 2 h, 4 h). Finally, the radioactivity of samples

was evaluated using gamma counter, and all relevant results were expressed as a percentage of injected dosage over weight of tissues in grams (%ID/g).

### Blood retention of <sup>99m</sup>Tc-complex in mice

The three studied <sup>99m</sup>Tc-complexes (200 µL, 14.8 MBq) were intravenously injected into the tail vein of mice. Blood sample of 10 µL were collected from mice and analyzed using a gamma counter at various post-injection time points (2, 15, and 30 minutes, and 1, 2, 4, 6, 8, 12, 16, and 24 hours). Results were shown as %ID/g.

### Statistical analysis

All statistical analyses were performed with SPSS 18.0 software (Chicago, Illinois, USA). Data are presented in the form of mean ± standard deviation (SD). The two-tailed student's *t*-test or one-way analysis of variance (ANOVA) was used to analyze differences in continuous variables among groups. Categorical or counted data were compared and analyzed using the chi-square test. *P*<0.05 provided evidence of statistical significance.

## Results

### Physicochemical evaluation of complexes

#### Stability

Three types of <sup>99m</sup>Tc-complexes including <sup>99m</sup>Tc-2-ntm-IDA, <sup>99m</sup>Tc-5-ntm-IDA, and <sup>99m</sup>Tc-5-ntm-asp all exhibited high stability (0.915±0.04, 0.935±0.012, and 0.950±0.023 respectively, Table 1) when they were evaluated in PBS solutions. We concluded that <sup>99m</sup>Tc-2-ntm-IDA, <sup>99m</sup>Tc-5-ntm-IDA, and <sup>99m</sup>Tc-5-ntm-asp were all stable at this temperature for at least 4 hours in PBS solutions *in vitro*. Besides that, we also studied the stability of these complexes in human plasma. As shown in Figure 4, dissociation or decomposition of these three complexes was rarely detected after 4-hour incubation.

#### Lipophilicity

As shown in Table 1, we also measured the partition coefficient between water and octanol. The  $\text{Log } P_{o/w}$  of 5-ntm-asp (−0.72±0.05) was much lower than that of 2-ntm-IDA (0.47±0.03) and 5-ntm-IDA (0.38±0.02) (*P*<0.05). This trend was associated with different structures of the three complexes since the lipophilicity was decreased by using asparagine units.

**Table 1.** Some physicochemical properties of developed Tc-complexes.

Complex	Stability in PBS%	Log P	Protein binding%
2-ntm-IDA	91.5±4.0	0.47±0.03	24.7±5.2
5-ntm-IDA	93.5±1.2	0.38±0.02	13.2±3.3
5-ntm-asp	95.0±2.3	-0.72±0.05	15.2±4.7

2-ntm-IDA – 2-nitroimidazole-iminodiacetic acid; 5-ntm-IDA – 5-nitroimidazole-iminodiacetic acid;  
 5-ntm-asp – 5-nitroimidazole-asparagine.

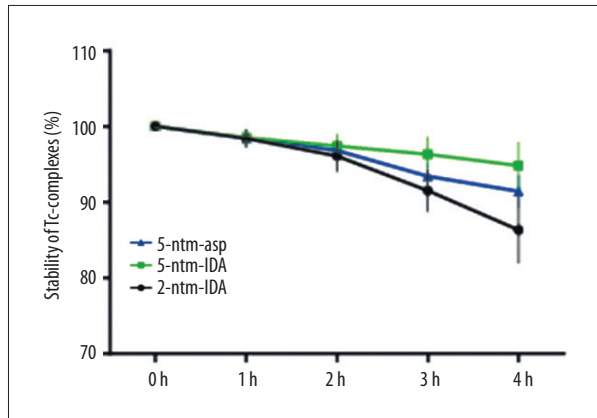


**Figure 4.** Stability of <sup>99m</sup>Tc-complexes in human plasma. Data are presented as mean ±SD for three independent experiments.

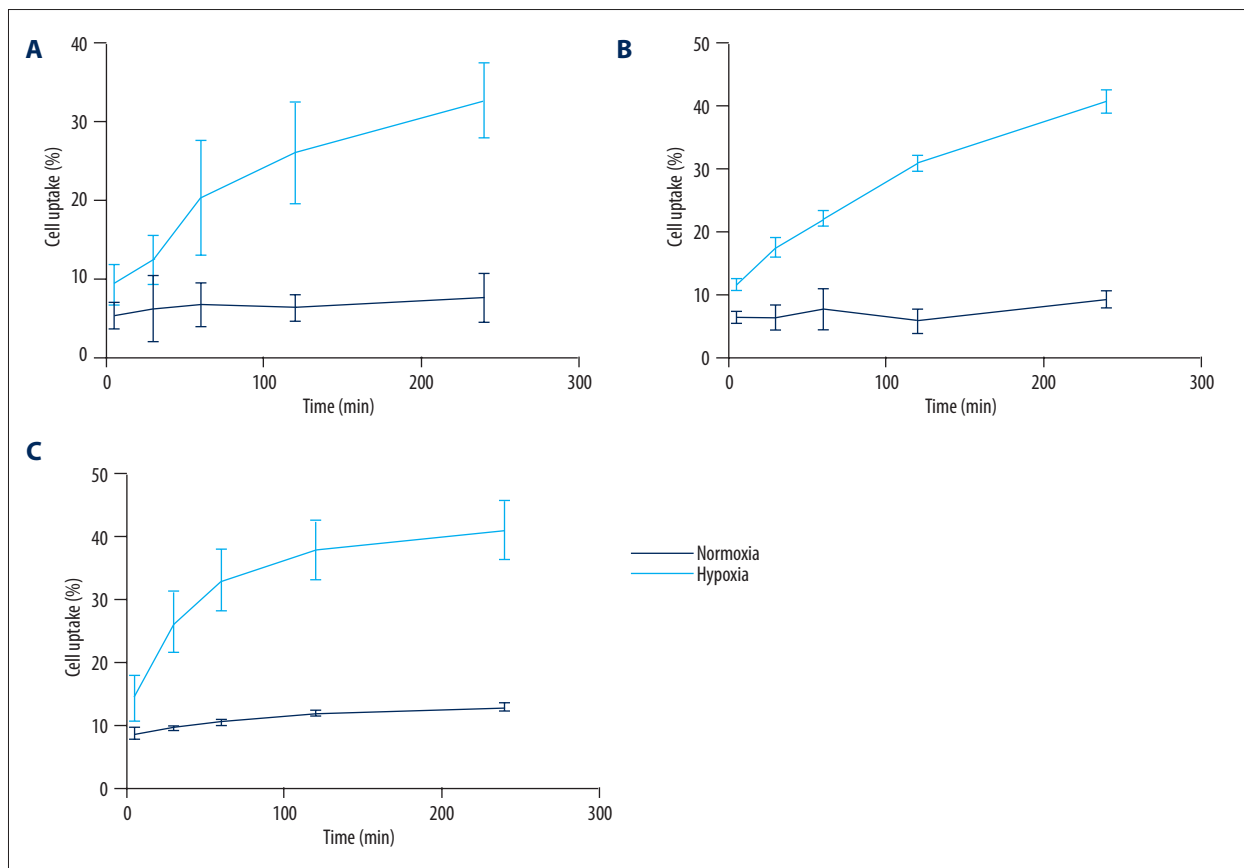


**Figure 5.** Blood retention curve of <sup>99m</sup>Tc-complexes. Data are presented as mean ±SD for three independent experiments.



**Table 2.** Accumulation of Tc-complexes in cells under hypoxic/aerobic conditions.

Complex	2-ntm-IDA		5-ntm-IDA		5-ntm-asp	
	Aerobic	Hypoxic	Aerobic	Hypoxic	Aerobic	Hypoxic
5 min	5.36±1.69	9.31±2.53	6.25±0.98	11.49±0.98	8.7±0.73	13.87±4.19
0.5 h	6.22±4.22	12.45±3.09	6.26±1.96	17.48±1.63	9.5±0.55	26.28±4.93
1 h	6.82±2.81	20.34±7.32	7.61±3.27	22.04±1.30	10.3±0.55	32.85±4.93
2 h	6.32±1.68	26.04±6.48	5.71±1.96	30.96±1.30	11.67±0.54	37.78±4.74
4 h	7.57±3.09	32.64±4.78	9.14±1.30	40.90±1.96	12.58±0.73	40.87±4.74

### Protein binding

<sup>99m</sup>Tc-nitroimidazole complex exhibited a low rate of protein binding, which was related to adequate pharmacokinetics. As suggested by Table 1, the protein binding rate of 5-ntm-asp was 15.2±4.7, which was close to that of 5-ntm-IDA (13.2±3.3) but significantly lower than that of 2-ntm-IDA (24.7±5.2) ( $P<0.05$ ).

### Biological evaluation of complexes

#### Cell uptake studies

Cell uptake analysis of the three <sup>99m</sup>Tc-complexes was carried out using human lung cancer cell line A549 under both normoxia and hypoxia conditions. The propidium iodide viability test was used to ensure that the viability of cell line A549 was maintained above 90% under hypoxic conditions [12]. As shown in Figure 5 and Table 2, the cell uptake patterns appeared to be consistent among the three groups in which cells were incubated with the three types of <sup>99m</sup>Tc-complexes. The cell uptake status under normoxia conditions was leveled among all three groups, whereas the cell uptake status under hypoxia conditions was steadily increased over time across the three groups ( $P<0.05$ ). Moreover, cells under hypoxia conditions exhibited significantly higher cell uptake compared with those under normoxia conditions over the experiment ( $P<0.05$ ). Although cells incubated with <sup>99m</sup>Tc-5-ntm-asp exhibited a relatively higher cell uptake (40.87±4.74) at the end of the experiment compared with the other two groups, its cell uptake ratio between hypoxic and normoxia conditions was 3.25±0.08, which was lower than that of cells incubated with <sup>99m</sup>Tc-2-ntm-IDA (4.47±0.10) ( $P<0.05$ ). Furthermore, cells incubated with <sup>99m</sup>Tc-5-ntm-asp had higher cell uptake than those incubated with <sup>99m</sup>Tc-2-ntm-IDA or <sup>99m</sup>Tc-5-ntm-IDA when the experiment was carried out under normoxia conditions ( $P<0.05$ ). Therefore, we concluded that asparagine unit was likely to be associated with cell uptake status.

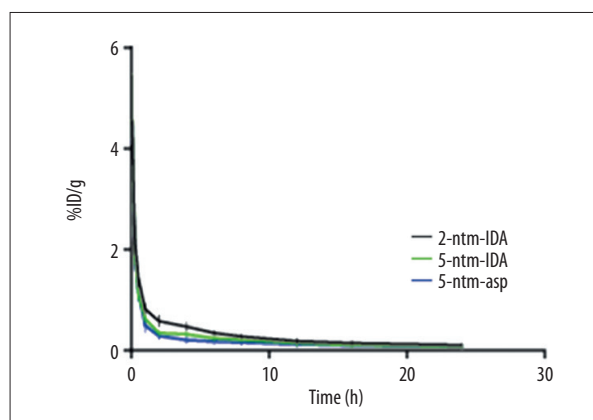


**Figure 6.** Accumulation status of <sup>99m</sup>Tc-2-ntm-IDA (A), <sup>99m</sup>Tc-5-ntm-IDA (B), and <sup>99m</sup>Tc-5-ntm-asp (C) in A549 cells under hypoxic/aerobic conditions. Data are presented as mean ±SD for three independent experiments.

#### Blood retention pattern in mice

The blood retention patterns were consistent across the three types of <sup>99m</sup>Tc-complexes. Blood retention patterns of the three studied <sup>99m</sup>Tc-complexes acted in accordance with a typical clearance pattern for small molecule compounds, in which fast rise and rapid washout of radioactivity were featured. The 2-ntm-IDA with higher  $\text{Log}P_{o/w}$  was associated with slower blood clearance compared to the other two complexes, which had lower  $\text{Log}P_{o/w}$ , suggesting that blood retention status may be related to lipophilicity of complexes (Figure 6).

#### Bio-distribution of <sup>99m</sup>Tc-complex in model mice

We conducted bio-distribution analysis in tumor-induced mice at 0.5, 2, and 4 hours after the three types of <sup>99m</sup>Tc-complexes were injected into mice. As shown in Figure 7, the uptake amount measured for each organ was expressed as percentage of dose per organ. For all three <sup>99m</sup>Tc-complexes, the intestine exhibited an obviously higher uptake percentage than other tissues, and this excessive uptake identified in the intestine was followed by those in liver as well as kidney ( $P<0.05$ ). This

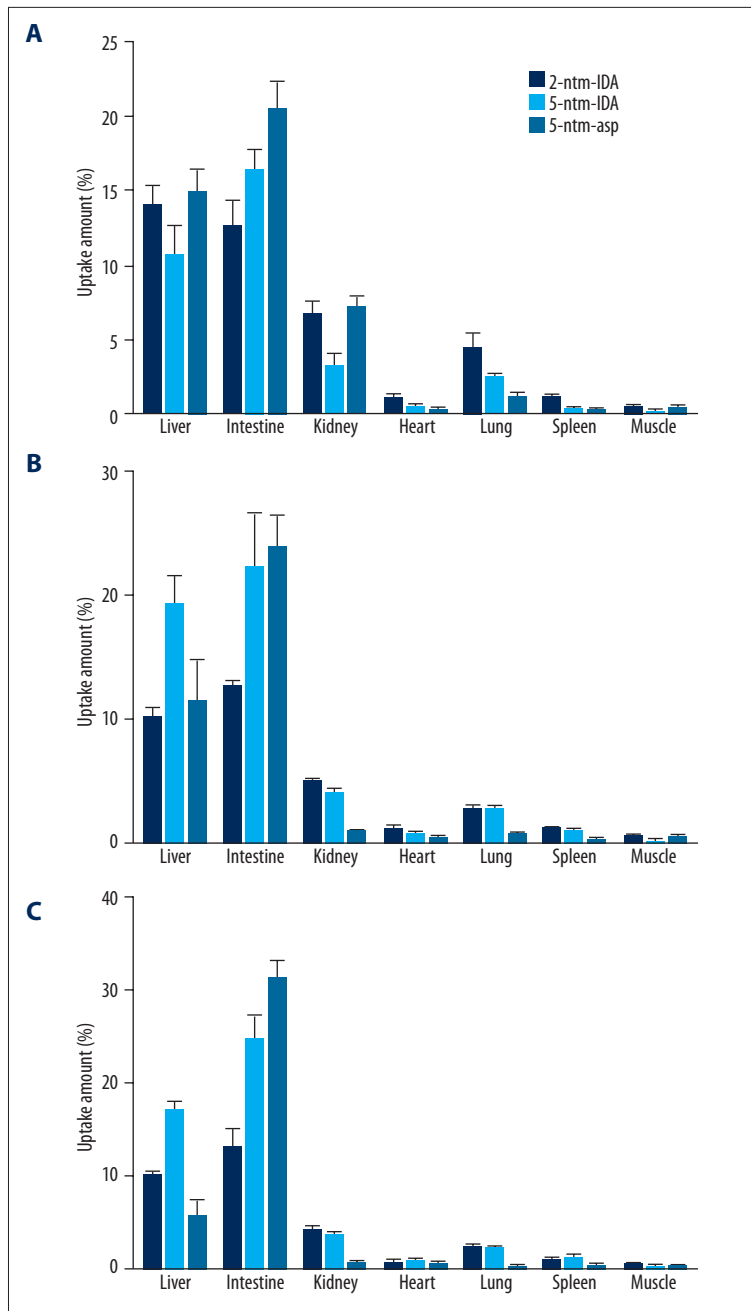


**Figure 7.** Biodistribution patterns of <sup>99m</sup>Tc-2-ntm-IDA, <sup>99m</sup>Tc-5-ntm-IDA, and <sup>99m</sup>Tc-5-ntm-asp complexes within mice 30 min (A), 2 h (B), and 4 h (C) after injections.

evidence suggested that these complexes were mainly excreted from the intestinal and urinary systems. By contrast, other organs including heart, lung, and spleen exhibited much lower uptake levels ( $P < 0.05$ ). It was also suggested by T/NT (Table 3) that 5-ntm-ASP was associated with the highest T/NT regarding such organs as heart, lung, spleen, and kidney when compared with 2-ntm-IDA and 5-ntm-IDA at 2 h and 4 h, respectively, after injections. Besides, T/liver of 5-ntm-ASP was always higher than that of 5-ntm-IDA at each detected time point (i.e., 30 min, 2 h, and 4 h). Figure 8 and Table 4 reveals the uptake status of blood and tumor *in vivo*, as well as the uptake ratio

between tumor and blood. For the synthesized <sup>99m</sup>Tc-5-ntm-asp, we discovered a desirable tumor uptake status ( $1.02 \pm 0.10$ ) along with a lower blood uptake ( $0.65 \pm 0.11$ ) when the experiment had been performed for 30 minutes. Apart from that, synthesized <sup>99m</sup>Tc-5-ntm-asp exhibited a significantly higher uptake ratio between tumor and blood compared with the other two complexes ( $P < 0.05$ , Figure 8, Table 4). Although approximately 60% of the uptake of the complexes was cleared in tumor in 2 hours, the activity appeared to be remarkable at all time points over the experiment. The uptake ratio between tumor and blood for all three complexes was increased as the

**Table 3.** Comparison of T/NT among <sup>99m</sup>Tc-5-ntm-asp, <sup>99m</sup>Tc-2-ntm-IDA and <sup>99m</sup>Tc-5-ntm-IDA within tumors of BALB/c nude mice.

Type	30 min			2 h			4 h		
	2-ntm-IDA	5-ntm-IDA	5-ntm-asp	2-ntm-IDA	5-ntm-IDA	5-ntm-asp	2-ntm-IDA	5-ntm-IDA	5-ntm-asp
T/Liver	0.07±0.01	0.04±0.01	0.07±0.01	0.07±0.01	0.03±0.01	0.03±0.01	0.07±0.01	0.02±0.00	0.05±0.01
T/Intestine	0.08±0.01	0.03±0.01	0.05±0.01	0.06±0.01	0.02±0.00	0.01±0.00	0.05±0.01	0.01±0.00	0.01±0.00
T/Kidney	0.15±0.02	0.14±0.03	0.14±0.04	0.15±0.03	0.12±0.02	0.36±0.03	0.17±0.02	0.10±0.02	0.50±0.02
T/Heart	0.82±0.09	0.81±0.08	3.09±0.08	0.74±0.07	1.07±0.09	1.18±0.07	1.16±0.07	0.51±0.03	2.17±0.15
T/Lung	0.21±0.02	0.18±0.01	0.84±0.07	0.28±0.02	0.19±0.02	0.67±0.03	0.30±0.01	0.17±0.02	2.60±0.18
T/Spleen	0.87±0.08	1.35±0.11	4.25±0.36	0.79±0.06	0.60±0.04	2.75±0.19	0.86±0.03	0.38±0.02	3.25±0.27
T/Muscle	1.85±0.14	2.00±0.18	1.76±0.15	2.25±0.21	3.43±0.31	1.57±0.09	2.58±0.17	2.92±0.21	1.86±0.10

T – tumor; NT – non-tumor.

experiment time extended from 30 minutes to 4 hours, and this trend was associated with fast blood clearance.

## Discussion

Tumor hypoxia is closely related to the deterioration of proliferate conditions, and it is usually followed by anatomically and functionally intrusive microcirculation [13]. The existence of hypoxic regions has negative impact on clinical therapy since tumor hypoxia is able to trigger resistance to both radiotherapy and chemotherapy. Moreover, tumor hypoxia is believed to be related to malignant progression and metastasis of cancer [14–17].

A large number of research studies have been dedicated to unveiling the biological behavior of nitroimidazoles in hypoxic tissues, and they provided solid evidence that the nitroimidazole ligand is degraded by enzyme and captured in hypoxic cells [18]. Nitroimidazoles undergo a variety of enzymatic one-electron decreases in hypoxic cells, and their metabolic products are merged for cell compositions. This decrease is more severe in cells with normal oxygen status, and consequently no tracer is accumulated [19]. This feature of nitroimidazole could be specifically applied to target hypoxic cells. Meanwhile, it is feasible to stably label molecules at relatively low ligand concentration of compounds *in vivo* with the introduction of [<sup>99m</sup>Tc(CO)<sub>3</sub>(H<sub>2</sub>O)<sub>3</sub>]<sup>+</sup> core [20,21]. This core expedites the formation of stable compounds with tridentate ligands including IDA, which facilitates protein refold and its metal-chelate affinity purification [22].

We discovered that <sup>99m</sup>Tc-5-ntm-asp had a more desirable stability and protein-binding rate, and a lower Log P<sub>o/w</sub> in PBS or human serum compared with <sup>99m</sup>Tc-2-ntm-IDA and <sup>99m</sup>Tc-5-ntm-IDA, and this trend may be explained by the introduction

of asparagine ligand, which is associated with a lower lipophilicity [23,24]. Theoretically, low protein binding is essential to the pharmacokinetics effectiveness that is contributed by potential radiopharmaceuticals [8]. In addition, only the free fraction of the radiotracer is able to penetrate cells and other biomembranes [7]. Moreover, molecules with higher lipophilicity are known to have higher serum binding, which contributes to slower clearance from blood, and this is consistent with our results indicating that <sup>99m</sup>Tc-2-ntm-IDA had the longest blood retention time [1]. On the other hand, <sup>99m</sup>Tc-5-ntm-asp is cleared faster from blood compared with other compounds, and this confirmed its more favorable biological evaluation [5]. In practice, relatively low lipophilicity accelerated the clearance of compound and supplied a more desirable tumor/background ratio [25].

Results from the *in vitro* experiment showed that the absorption values of the three compounds slightly changed under aerobic conditions over the experiment, while they were significantly increased over time under hypoxic conditions. The 2-nitroimidazole compounds exhibited relatively higher uptake status under hypoxia circumstances, for they readily obtained electrons to form radical anions, which were able to irreversibly bind with cellular components under anoxic conditions [4]. Furthermore, Chu et al. demonstrated that 5-nitroimidazoles, which have lower avidity with electrons than 2-nitroimidazole, could not be effectively decreased and reserved in hypoxia cells [3,25]. However, although <sup>99m</sup>Tc-5-ntm-asp had a lower aerobic/hypoxic absorption ratio in comparison with <sup>99m</sup>Tc-5-ntm-IDA, <sup>99m</sup>Tc-5-ntm-asp more quickly reached the plateau of hypoxic uptake than <sup>99m</sup>Tc-5-ntm-IDA, which meant that <sup>99m</sup>Tc-5-ntm-asp could satisfy the demand for cell uptake more effectively.

As suggested by the bio-distribution experiment, all three compounds exhibited the highest uptake status in intestine,

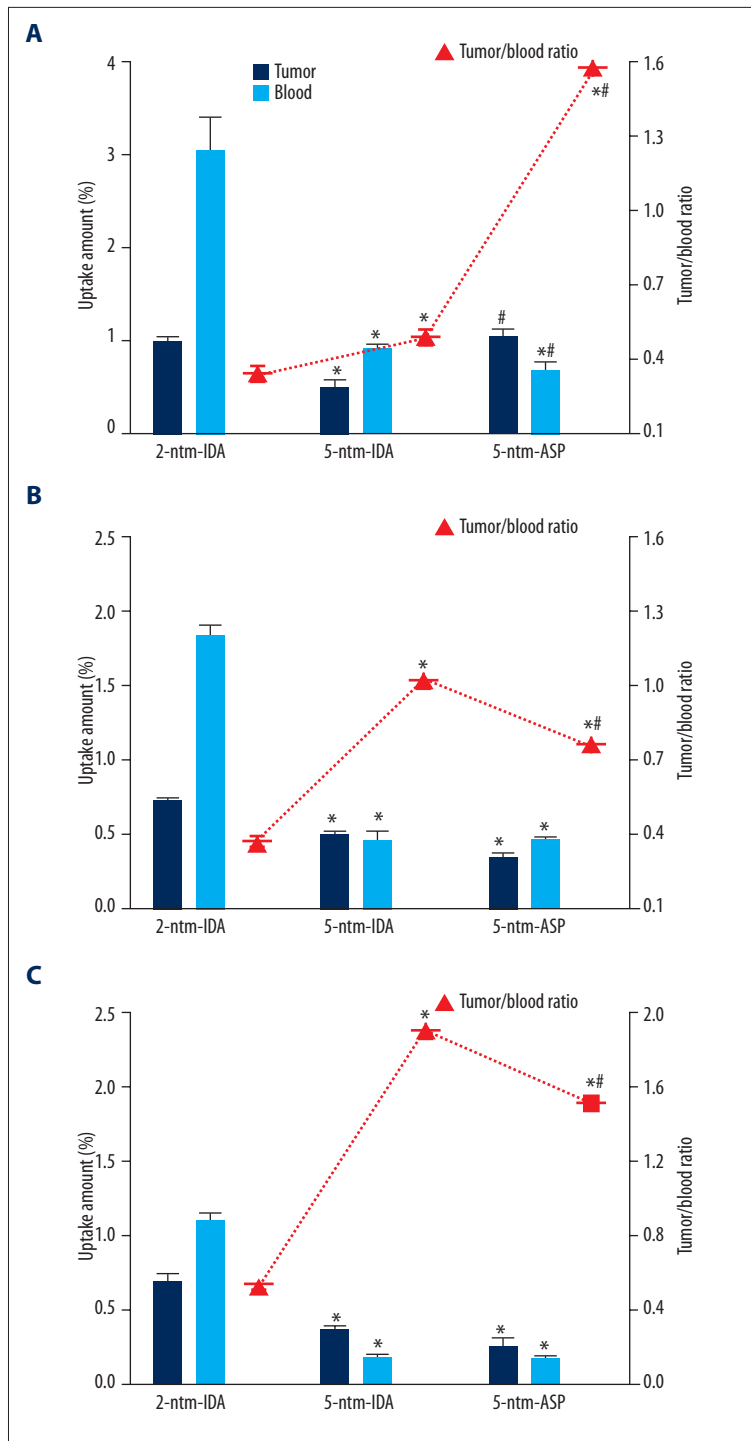


**Figure 8.** Tumor to blood ratio obtained with <sup>99m</sup>Tc-2-ntm-IDA, <sup>99m</sup>Tc-5-ntm-IDA, and <sup>99m</sup>Tc-5-ntm-asp complexes within mice 30 min (A), 2 h (B), and 4 h (C) after injections. \* Indicates <0.05 compared with <sup>99m</sup>Tc-2-ntm-IDA; # indicates <0.05 compared with <sup>99m</sup>Tc-5-ntm-IDA.

liver, and kidney, indicating that these compounds were mainly excreted from the intestinal and urinary systems [10]. Lipophilicity, other than ligand density of compounds, has been suggested to provide convincing evidence for the bio-distribution of compounds in several organs, including liver and kidney [7,26–28]. It was noteworthy that higher T/NT values were closely linked with more desirable imaging results.

When compared with 2-ntm-IDA and 5-ntm-IDA at 2 h and 4 h, respectively, after injection of the compounds, 5-ntm-asp remained associated with the highest T/NT regarding such organs as heart, lung, spleen, and kidney. Besides, T/NT of 5-ntm-asp was always higher than that of 5-ntm-IDA at each detected time point, when liver was considered. In addition, since <sup>99m</sup>Tc-2-ntm-IDA has the highest lipophilicity compared with

**Table 4.** Tumor to blood ratio obtained with Tc-complexes at various time points.

Organ or ratio	30 min			2 h			4 h		
	2-ntm-IDA	5-ntm-IDA	5-ntm-asp	2-ntm-IDA	5-ntm-IDA	5-ntm-asp	2-ntm-IDA	5-ntm-IDA	5-ntm-asp
Blood	3.03±0.38	0.89±0.06	0.65±0.11	1.83±0.08	0.45±0.06	0.44±0.02	1.08±0.07	0.18±0.02	0.17±0.02
Tumor	0.96±0.07	0.46±0.10	1.02±0.10	0.72±0.01	0.48±0.03	0.33±0.04	0.67±0.06	0.35±0.03	0.26±0.05
Tumor/blood	0.32±0.01	0.52±0.07	1.57±0.02	0.39±0.01	1.07±0.02	0.75±0.01	0.62±0.01	1.94±0.02	1.55±0.03
Tumor/muscle	1.85±0.07	2.00±0.06	4.65±0.07	2.23±0.04	3.43±0.05	1.07±0.02	2.56±0.02	2.88±0.05	3.29±0.07

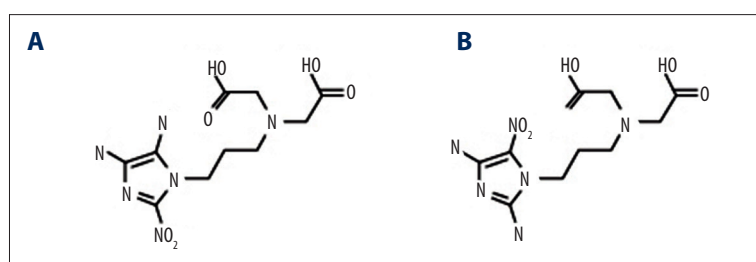
other two compounds, its fast accumulation further contributed to the lowest tumor/blood uptake ratio. On the contrary, at 30 min after injection, 5-ntm-asp obtained a relatively high tumor/blood ratio that was just slightly lower than the tumor/blood ratio of 5-ntm-IDA at 4 hours after injection, suggesting that application of 5-ntm-asp could contribute to a desirable imaging within 30 min, one-eighth of 4 h for similar results in the application of 5-ntm-IDA.

Nevertheless, <sup>99m</sup>Tc-nitroimidazoles have one underlying limitation since they are unable to cope with the entire population of hypoxic cells. It is advised that the entire population of target cells should be labeled using nuclear medicine techniques in order to obtain an accurately quantitative measurement of tumor hypoxia. Underestimation of the hypoxic fraction may occur if low-dosage radiotracers are metabolically depleted from organs or tissues before the target population of cells is reached [29]. Another limitation of this study lay in its selection of tumor cells since only A549 cells were used. Different tumor cells were supposed to be compared in their uptakes of asparagines, in which way effects imposed by types of tumor cells could be removed.

## Conclusions

This study comprehensively synthesized and assessed several imaging agents for tumor hypoxia, including <sup>99m</sup>Tc-2-ntm-IDA, <sup>99m</sup>Tc-5-ntm-IDA, and <sup>99m</sup>Tc-5-ntm-asp. We concluded that <sup>99m</sup>Tc-5-ntm-asp exhibited relatively high stability *in vitro* and *in vivo*, as well as a favorable hypoxic/aerobic ratio, though not better than that of <sup>99m</sup>Tc-5-ntm-IDA. Besides that, <sup>99m</sup>Tc-5-ntm-asp had more effective pharmacokinetics than those of <sup>99m</sup>Tc-2-ntm-IDA and <sup>99m</sup>Tc-5-ntm-IDA, and this superiority may be attributed to its lower lipophilicity with the introduction of asparagine ligand. In summary, despite certain shortcomings, 5-ntm-asp could serve as a complementary imaging agent to 5-ntm-IDA for tumor hypoxia, and development of novel imaging agents could use its strength for reference. However, relevant characteristics of 5-ntm-ASP should be further improved before it is put into clinical usage.

## Supplementary Figure



**Supplementary Figure 1.** The structures of 2-ntm-IDA (A) and 5-ntm-IDA (B).

## References:

- Mallia MB, Subramanian S, Mathur A et al: A study on nitroimidazole-<sup>99m</sup>Tc(CO)<sub>3</sub> complexes as hypoxia marker: Some observations towards possible improvement in *in vivo* efficacy. *Nucl Med Biol*, 2014; 41: 600–10
- Chu T, Li R, Hu S, Liu X, Wang X: Preparation and biodistribution of technetium-99m-labeled 1-(2-nitroimidazole-1-yl)-propanhydroxyiminoamide (N2IPA) as a tumor hypoxia marker. *Nucl Med Biol*, 2004; 31: 199–203
- Chu T, Hu S, Wei B et al: Synthesis and biological results of the technetium-99m-labeled 4-nitroimidazole for imaging tumor hypoxia. *Bioorg Med Chem Lett*, 2004; 14: 747–49
- Huang H, Zhou H, Li Z et al: Effect of a second nitroimidazole redox centre on the accumulation of a hypoxia marker: Synthesis and *in vitro* evaluation of <sup>99m</sup>Tc-labeled bisnitroimidazole propylene amine oxime complexes. *Bioorg Med Chem Lett*, 2012; 22: 172–77

- Zhang Q, Huang H, Chu T: *In vitro* and *in vivo* evaluation of technetium-99m-labeled propylene amine oxime complexes containing nitroimidazole and nitrotriazole groups as hypoxia markers. *J Labelled Comp Radiopharm*, 2016; 59: 14–23
- Evans SM, Kachur AV, Shiu CY et al: Noninvasive detection of tumor hypoxia using the 2-nitroimidazole [<sup>18</sup>F]EF1. *J Nucl Med*, 2000; 41: 327–36
- Giglio J, Dematteis S, Fernandez S et al: Synthesis and evaluation of a new <sup>99m</sup>Tc(I)-tricarbonyl complex bearing the 5-nitroimidazol-1-yl moiety as potential hypoxia imaging agent. *J Labelled Comp Radiopharm*, 2014; 57: 403–9
- Giglio J, Fernandez S, Pietzsch HJ et al: Synthesis, *in vitro* and *in vivo* characterization of novel <sup>99m</sup>Tc-<sup>4+1</sup>-labeled 5-nitroimidazole derivatives as potential agents for imaging hypoxia. *Nucl Med Biol*, 2012; 39: 679–86
- Bartholoma MD, Louie AS, Valliant JF, Zubieta J: Technetium and gallium derived radiopharmaceuticals: Comparing and contrasting the chemistry of two important radiometals for the molecular imaging era. *Chem Rev*, 2010; 110: 2903–20
- Li N, Zhu H, Chu TW, Yang Z: Preparation and biological evaluation of (<sup>9</sup>)<sup>99m</sup>Tc-N4IPA for single photon emission computerized tomography imaging of hypoxia in mouse tumor. *Eur J Med Chem*, 2013; 69: 223–31
- Fernandez S, Giglio J, Rey AM, Cerecetto H: Influence of ligand denticity on the properties of novel (<sup>9</sup>)<sup>99m</sup>Tc(I)-carbonyl complexes. Application to the development of radiopharmaceuticals for imaging hypoxic tissue. *Bioorg Med Chem*, 2012; 20: 4040–48
- Suzuki T, Fujikura K, Higashiyama T, Takata K: DNA staining for fluorescence and laser confocal microscopy. *J Histochem Cytochem*, 1997; 45: 49–53
- Johns RA, Takimoto E, Meuchel LW et al: Hypoxia-inducible factor 1alpha is a critical downstream mediator for hypoxia-induced mitogenic factor (FIZZ1/RELMalpha)-induced pulmonary hypertension. *Arterioscler Thromb Vasc Biol*, 2016; 36: 134–44
- Vaupel P, Mayer A: Hypoxia in cancer: Significance and impact on clinical outcome. *Cancer Metastasis Rev*, 2007; 26: 225–39
- Moeller BJ, Richardson RA, Dewhirst MW: Hypoxia and radiotherapy: Opportunities for improved outcomes in cancer treatment. *Cancer Metastasis Rev*, 2007; 26: 241–48
- Subarsky P, Hill RP: The hypoxic tumour microenvironment and metastatic progression. *Clin Exp Metastasis*, 2003; 20: 237–50
- Vaupel P: Hypoxia and aggressive tumor phenotype: implications for therapy and prognosis. *Oncologist*, 2008; 13(Suppl. 3): 21–26
- Riche F, d'Hardemare AD, Sepe S et al: Nitroimidazoles and hypoxia imaging: synthesis of three technetium-99m complexes bearing a nitroimidazole group: Biological results. *Bioorg Med Chem Lett*, 2001; 11: 71–74
- Krohn KA, Link JM, Mason RP: Molecular imaging of hypoxia. *J Nucl Med*, 2008; 49(Suppl. 2): 129S–48S
- Kim DW, Kim WH, Kim MH, Kim CG: Synthesis and evaluation of novel Tc-99m labeled NGR-containing hexapeptides as tumor imaging agents. *Labelled Comp Radiopharm*, 2015; 58: 30–35
- Schibli R, Alberto R, Abram U et al: Structural and (<sup>99</sup>)Tc NMR investigations of complexes with fac-[Tc(CO)(3)](+) moieties and macrocyclic thioethers of various ring sizes: Synthesis and x-ray structure of the complexes fac-[Tc(9-ane-S(3))(CO)(3)]Br, fac-[Tc(2)(tosylate)(2)(18-ane-S(6))(CO)(6)], and fac-[Tc(2)(20-ane-S(6)-OH)(CO)(6)][tosylate](2). *Inorg Chem*, 1998; 37: 3509–16
- Liu H, Dong X, Sun Y: Grafting iminodiacetic acid on silica nanoparticles for facilitated refolding of like-charged protein and its metal-chelate affinity purification. *J Chromatogr A*, 2016; 1429: 277–83
- Mfuh AM, Mahindaratne MP, Quintero MV et al: Novel asparagine-derived lipid enhances distearoylphosphatidylcholine bilayer resistance to acidic conditions. *Langmuir*, 2011; 27: 4447–55
- Kosky AA, Dharmavaram V, Ratnaswamy G, Manning MC: Multivariate analysis of the sequence dependence of asparagine deamidation rates in peptides. *Pharm Res*, 2009; 26: 2417–28
- Mei L, Wang Y, Chu T: (<sup>9</sup>)<sup>99m</sup>Tc/Re complexes bearing bisnitroimidazole or mononitroimidazole as potential bioreductive markers for tumor: Synthesis, physicochemical characterization and biological evaluation. *Eur J Med Chem*, 2012; 58: 50–63
- Schibli R, La Bella R, Alberto R et al: Influence of the denticity of ligand systems on the *in vitro* and *in vivo* behavior of (<sup>99m</sup>)Tc(I)-tricarbonyl complexes: A hint for the future functionalization of biomolecules. *Bioconjug Chem*, 2000; 11: 345–51
- Mallia MB, Subramanian S, Mathur A et al: On the isolation and evaluation of a novel unsubstituted 5-nitroimidazole derivative as an agent to target tumor hypoxia. *Bioorg Med Chem Lett*, 2008; 18: 5233–37
- Yang DJ, Ilgan S, Higuchi T et al: Noninvasive assessment of tumor hypoxia with <sup>99m</sup>Tc labeled metronidazole. *Pharm Res*, 1999; 16: 743–50
- Melo T, Tunggal JK, Ballinger JR, Rauth AM: Flux through multicellular layers of a technetium-99m-nitroimidazole for imaging hypoxia. *Cancer Biother Radiopharm*, 2002; 17: 515–26